

Dallinger, David; Link, Jochen; Büttner, Markus

Working Paper

Smart grid agent: Plug-in electric vehicle

Working Paper Sustainability and Innovation, No. S8/2013

Provided in Cooperation with:

Fraunhofer Institute for Systems and Innovation Research ISI

Suggested Citation: Dallinger, David; Link, Jochen; Büttner, Markus (2013) : Smart grid agent: Plug-in electric vehicle, Working Paper Sustainability and Innovation, No. S8/2013, Fraunhofer-Institut für System- und Innovationsforschung ISI, Karlsruhe

This Version is available at:

<https://hdl.handle.net/10419/87728>

Standard-Nutzungsbedingungen:

Die Dokumente auf EconStor dürfen zu eigenen wissenschaftlichen Zwecken und zum Privatgebrauch gespeichert und kopiert werden.

Sie dürfen die Dokumente nicht für öffentliche oder kommerzielle Zwecke vervielfältigen, öffentlich ausstellen, öffentlich zugänglich machen, vertreiben oder anderweitig nutzen.

Sofern die Verfasser die Dokumente unter Open-Content-Lizenzen (insbesondere CC-Lizenzen) zur Verfügung gestellt haben sollten, gelten abweichend von diesen Nutzungsbedingungen die in der dort genannten Lizenz gewährten Nutzungsrechte.

Terms of use:

Documents in EconStor may be saved and copied for your personal and scholarly purposes.

You are not to copy documents for public or commercial purposes, to exhibit the documents publicly, to make them publicly available on the internet, or to distribute or otherwise use the documents in public.

If the documents have been made available under an Open Content Licence (especially Creative Commons Licences), you may exercise further usage rights as specified in the indicated licence.

Working Paper Sustainability and Innovation
No. S 8/2013



David Dallinger
Jochen Link
Markus Büttner

Smart Grid Agent: Plug-In Electric Vehicle

Abstract

Abstract-This study describes a method for programming a plug-in electric vehicle agent that can be used in power system models and in embedded systems implemented in real plug-in electric vehicles. Implementing the software in real-life applications and in simulation tools enables research with a high degree of detail and practical relevance. Agent-based programming, therefore, is an important tool for investigating the future power system. To demonstrate the plug-in electric vehicle agent behavior, an optimization algorithm is presented and two battery aging methods as well as their effect on V2G operation are analyzed. Aging costs based on the depth of discharge result in shallow cycles and a strong dependency on driving behavior, because the state-of-charge affects the discharging process. In contrast, aging costs based on energy throughput calculations results in deeper cycles and V2G operation which is less dependent on driving behavior.

Table of Contents

	Page
1 Introduction	1
2 Method	2
3 Plug-in electric vehicle agent.....	3
3.1 Driving behavior	4
3.2 Battery degradation	6
3.2.1 Model based on the depth-of-discharge	8
3.2.2 Model based on energy throughput.....	9
3.2.3 Discharge costs.....	10
3.3 Optimization	11
4 Results	14
5 Conclusions.....	17
6 Acknowledgements	17
7 References.....	18

1 Introduction

Pure battery vehicles and plug-in hybrid vehicles are now available commercially to private consumers. Even though their mass market diffusion will certainly take a significant time, questions should be asked now about the challenges and chances emerging due to electric load and storage becoming available in the electricity system. To standardize communication, the ISO/IEC 15118 is currently being developed, a protocol that defines the information exchange between the charging point and the vehicle. This protocol covers the communication of price signals to the vehicle, but not the exchange of vehicle-specific data. Therefore it seems likely that smart charging schedules will be generated and optimized by algorithms used in the vehicle and not by a central operator. To optimize the charging and discharging schedule, information on the battery state and consumer needs is required that is only available within the vehicle. Therefore, a tariff-based demand response with vehicle-based optimization of the charging and discharging schedule seems to be a promising approach for realizing V2G applications. In this case relevant information to generate a smart charging schedule can remain in the vehicle and the communication of user- or battery-specific data is not necessary.

Several studies have addressed smart grid agents and tariff-based demand response. [1] presents an agent for a residential cooling system that receives a price signal, a 24 h rolling average price and the standard deviation of the price to generate a minimal cost operation schedule under temperature constraints. [2] defines control algorithms for storage, process shifting and demand reduction appliances. Autonomous plug-in electric vehicles (PEVs) frequency and voltage control is analyzed in [3]. The theory and implementation of multi-agent systems are discussed in [4], [5] and [6]. [7] and [8] present a multi-agent coordination concept that is implemented by [9] in a field test using different demand response devices. Based on simulations, [10] and [11] discuss the design of controls and incentives in smart grids. Design examples of indirect tariff-based control mechanisms including PEVs are presented for congestion pricing [12], [13] and managing a distributed grid energy hub [14]. A specific distributed optimization strategy for PEVs is defined in [15] and [16].

Similar to [15], the work presented here defines an optimization strategy for PEVs but also includes battery aging costs based on depth of discharge requiring nonlinear optimization. This optimization strategy was then implemented in

Volkswagen vehicles. Therefore, the method allows a realistic estimate of PEVs' operation controlled by ISO/IEC 15118 which is highly relevant for research. Additionally, a method to simulate driving behavior is included which provides necessary input parameters such as the vehicles' standing time. Including driving behavior allows the method to be used in power system models instead of deterministic driving data which is often not available.

The paper is structured as follows. Section 2 discusses the applied tariff-based control method. Section 3 then gives a detailed description of the PEVs' agent, including driving behavior (sub Section 3.1), battery aging (sub Section 3.2) and the optimization algorithm (sub Section 3.3). Finally, Section 4 describes the results of applying the PEVs' agent with different methods to calculate discharging costs and Section 5 concludes.

2 Method

The idea of agent-based simulation combines game theory, social sciences and software engineering. An agent is defined as: "... a computer system that is situated in some environment, and that is capable of autonomous action in this environment in order to meet its design objectives." [19]. Similar to a feedback loop in control theory, this includes a perception and action functionality. The perception function is used to observe the environment. In the context of power systems this could be a transformer station observing active and reactive power flows in the connected grid, or a distributed device such as a PEV observing the drivers' needs, battery state and incentives from the smart grid. The action function for PEVs would be charging or feeding electricity back to the grid. Providing reactive power and grid monitoring are other possible actions. To schedule the action of the agent, an optimization algorithm is applied here, considering all constraints on driving behavior, battery restrictions and consumer preferences (see Section 3).

The agent presented here was applied in the field trial "Flottenversuch Elektromobilität" by integrating an embedded system into a Volkswagen Golf Variant "TwinDrive" PEV [17]. Real-time prices can then be sent to the vehicles and the embedded PEVs' agent via the charging infrastructure.

Beside the functionality of agents, the management of the agents is also an important issue. The objective function of a single agent is not necessarily consistent with the objective of the grid or power system. For example, assuming that several devices optimize their electricity consumption according to one price

signal would result in a high simultaneousness of electricity consumption (see [20] and [21]). A mechanism design [22] or control mechanism is necessary to avoid this unwanted result.

A mechanism design for the presented agent was implemented in the electricity market and system model PowerACE [23]. PowerACE is a marginal cost-based simulation model focusing on electricity markets and electricity generation from renewable energy sources. To control many PEVs' agents acting in the PowerACE model, a two-stage mechanism design based on dynamic pricing is used [18]. In the first stage, a price forecast $p(t)_{pool}$ of market clearing prices is applied for a specific pool of PEVs. In the second stage, a variable grid fee $p(t)_{gridfee}$ is added. Applying this method of individual real-time pricing results in slightly different price signals for every agent. The differences are detected by the optimization algorithm and result in an optimal residual load valley filling. From a consumer perspective, differences are very small, but still result in a non-equal trading of electricity consumers which is not permitted under the current legal conditions.

Other applications of the mechanism design are also possible such as optimizing a micro-grid or balancing the generation forecast errors of fluctuating generation sources. However, the control of such agents is not considered in this study, which only focuses on the PEVs' software agent.

3 Plug-in electric vehicle agent

Besides receiving a price or control signal, the PEVs' agent consists of two additional perception functionalities necessary to make the charging or V2G decision as given in Figure 3-1.

First, information about the driving behavior of the vehicle is required. The driving behavior defines the standing time and the objective status of the state-of-charge. In practice, the information on user preferences is transmitted via a user interface in the vehicle. After each trip, users can define the time to the next trip (grid management time) and the state of charge (soc) necessary. In the presented simulation model, driving behavior data are generated using a probability-based approach and are known in advance. This implies that users perfectly plan their driving behavior. The simulation of the driving behavior is explained in Section 3.1.

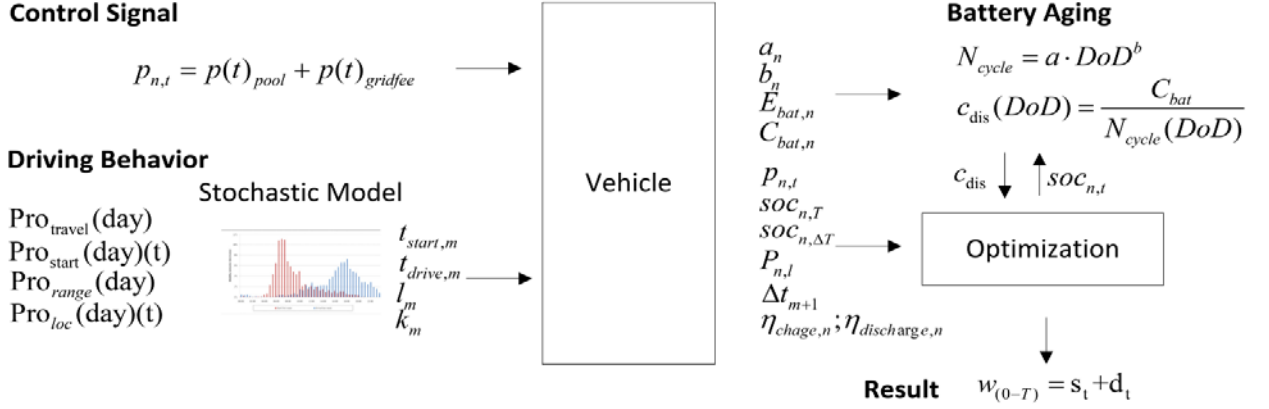
Plug-In Electric Vehicle- Agent:

Figure 3-1: Overview of Plug-In Electric Vehicle Agent

Second, PEVs providing V2G must consider discharging costs. The discharging costs consist of the efficiency or losses due to a charging and discharging cycle and battery degradation. The main focus here is on the battery degradation costs, but the approach can also include profit contribution or parameters for strategic bidding. Two approaches are applied to calculate the battery degradation costs: an energy throughput and a depth of discharge method (see Section 3.2).

Beside the perception functions, an optimization algorithm is necessary to decide on the charging or discharging schedule. To calculate the operation schedule, a graph search algorithm is used allowing nonlinear battery degradation, which is explained in Section 3.3.

3.1 Driving behavior

Driving behavior is modeled using the probabilities introduced in [20] and given for different mobility surveys in [18]. The flow diagram in Figure 3-2 shows the stochastic process to generate trips.

The driving behavior simulation starts before the energy-related simulation and the next trip is already known when returning from the current trip (i.e. perfect foresight).

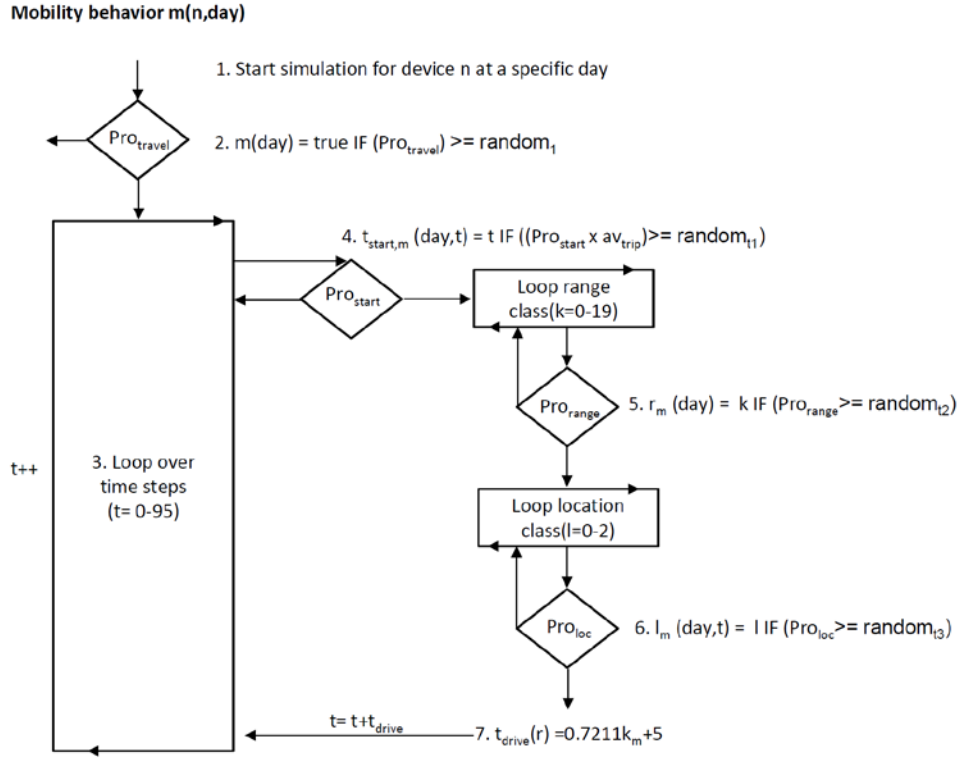


Figure 3-2: Stochastic simulation process of mobility behavior

At t_{start} the beginning of the simulation process for a single device n a first random value is used to determine if the vehicle starts a trip on the specific day ($Prob_{travel}$) (see step 2 in Figure 3-2). If this is not the case, the simulation continues with the next vehicle. If the vehicle starts a trip m , the probability to start a trip Pro_{start} multiplied by the average trips per day over all time steps is verified (step 4 in Figure 3-2).

The values of $random_{t,1-3}$ (see Figure 3-2) are renewed after each time step t . The value of $random_1$ is set by the Java random function before the loop over all time steps of the day.

For the start of a trip, probabilities for the range r ($Prob_{range}$) and location l ($Prob_{loc}$) are retrieved and assigned to the trip (steps 5 and 6 in Figure 3-2). To distinguish the distance k_m to be driven within the range classification k , a random value is subtracted by k . The driving time of the trip m , $t_{drive,m}$ is calculated according to the linear function [18]

$$t_{drive,m}(k) = 0.7211 k_m + 5 \quad (1)$$

and added to the time steps of the counting variable (step 7 in Figure 3-2) of the loop over all time steps. If no start time is assigned within T , the number of the trips is 1 and the start probability is retrieved until a start time is determined.

To calculate the operation schedule of the PEV agent, the following mobility parameters are necessary:

- The energy used during the trip to calculate the state of charge soc after the current trip:

$$soc_{n,t+t_{drive}} = soc_{n,t} - \frac{k_m \cdot \eta_{k_m}}{E_{bat}} \quad (2)$$

Here, η_{km} is the efficiency of converting electrical into mechanical energy.

- The start time of the current $t_{start,m}$ and next trip $t_{start,m+1}$ as well as the driving time $t_{drive,m}$ to define the grid management time Δt_m (period of optimization):

$$\Delta t(m) = (t_{start,m+1} - t_{start,m}) - t_{drive,m} \quad (3)$$

- The energy necessary for the next trip to calculate the objective status of the soc at the end of the optimization time period.

$$soc_{n,\Delta t} = \frac{k_{m+1} \cdot \eta_{km}}{E_{bat}} \quad (4)$$

Alternatively, an objective soc of 100 % can be used.

3.2 Battery degradation

Information about the wear of vehicle batteries is needed as a decision-making aid for feeding back electricity into the grid. In this chapter, battery degradation is discussed with regard to finding a simplified approach to model battery wear. In the following section, lithium-ion batteries are addressed in general without distinguishing the broad variety of lithium-ion battery chemistries and their specific characteristics.

Battery aging refers to irreversible physical and chemical effects that reduce battery performance. The end-of-life of automotive batteries is defined as a nominal capacity fade of 80 % compared to the initial rated capacity [24]. The capacity fade of lithium batteries is mainly influenced by the following stress factors [25], [26] and [27]:

- Temperature
- Cycles
- State-of-charge swing
- C-rate
- Waiting periods
- Soc in waiting periods.

The calendar life of batteries is mostly determined by thermal aging. An increase in temperature augments the relative cell resistance over time and reduces the lifetime [28]. The relevance of temperature for V2G is reduced if battery pre-cooling or pre-heating is assumed before beginning a V2G cycle. If conditions are too harsh, cycling could be restricted. During discharging, it is assumed that the cooling system is able to keep the temperature within the defined levels. Hence, temperature-related calendar life is only an issue if no grid connection is available and does not apply to cycling under conditions that can be defined to limit battery aging.

The c-rate or discharging and charging power affects age-ing and influences cell temperature. For example, [29] defines aging factors for specific c-rates. In terms of V2G cycles, the c-rate is very low compared to driving cycles. The rated power of a PEV motor ranges from 30 to 100 kW with correspondingly higher peak power, whereas the power used in a V2G cycle is in the range of 3 to 20 kW at a standard home grid connection. In terms of LiFe-PO₄ cell chemistry, [29] found that the capacity fading factor for driving (2.85 C-rate) is 2.2 times higher than for V2G (0.5 C-rate).

The cycle life related to the depth-of-discharge (DoD) or soc-swing is described in various publications (e.g. [30] and [31] and given by battery manufacturers for batteries under test conditions. Most experts describe this relation as one of the main factors for cycle-based battery aging, even if the influence of this factor seems to be rather low for LiFePO₄-based chemistries [29].

The influence of the stress factors on battery aging varies for different lithium-based battery chemistries. Furthermore, cell dimensions and system design play an important role for the lifetime [26]. Modeling physical and chemical processes yields the most accurate information about battery aging but also has the highest complexity (e.g. [27]). Laboratory experiments are necessary to characterize each specific battery chemistry. This was not feasible for this re-

search study and algorithms are too complex to run in a vehicle-embedded system.

Weighted energy throughput or Ah models are less complex and can be used as an accurate heuristic approach to determine battery aging [27]. Detailed information about the effects of different stress factors is required. Because lithium-based battery chemistries are undergoing rapid development, the relevant information is not readily available and it is still unclear which will be the dominant materials used in the future, so it is hard to define these factors. A related approach which simply takes one stress factor into account is the event-oriented aging model or Wöhler curve [27].

This approach is used to determine the number of cycles of a battery as a function of the depth-of-discharge until the end of its lifetime. For V2G cycles where it is possible to define cycling conditions (temperature, c-rate, waiting periods etc.), cycle life related to the depth-of-discharge seems to be adequate for modeling V2G in the electricity sector. In addition, this approach can be adapted to model degradation costs for future scenarios considering batteries with a better cycle life performance. To account for a lower influence of the DoD, a model based on the energy throughput with parameters published in [29] is also used and compared to the common DoD functions.

3.2.1 Model based on the depth-of-discharge

According to [32] and [33], battery degradation is influenced by the depth-of-discharge (see Figure 3-3). The cycle life N_{cycle} dependent on the soc-swing is referred to as the depth-of-discharge DoD and can be described by Eq. 5.

$$N_{cycle} = a \cdot DoD^b \quad (5)$$

For a currently available Li-ion battery, parameters $a_{Saft}=1331$ and $b_{Saft}=-1.825$ are used. The parameters result from a trend line drawn from data given by [33] for a high energy cell manufactured by the company Saft. In general, the performance of a single cell is better than the entire battery system because of non-uniform degradation. The cell performance is simplified here. The U.S. Advanced Battery Consortium (USABC) goal is the basis for estimating the degradation of future battery systems [34]. In this case the parameters result in $a_{USABC}=2744$ and $b_{USABC}=-1.665$. Here, a very optimistic 2030 scenario is assumed with the parameters $a_{Scenario2030}=4000$ and $b_{Scenario2030}=-1.632$. Figure 3-3

summarizes the data used and shows the performance of a nickel-metal hydride (NiMH) battery and manufacturer values as a reference.

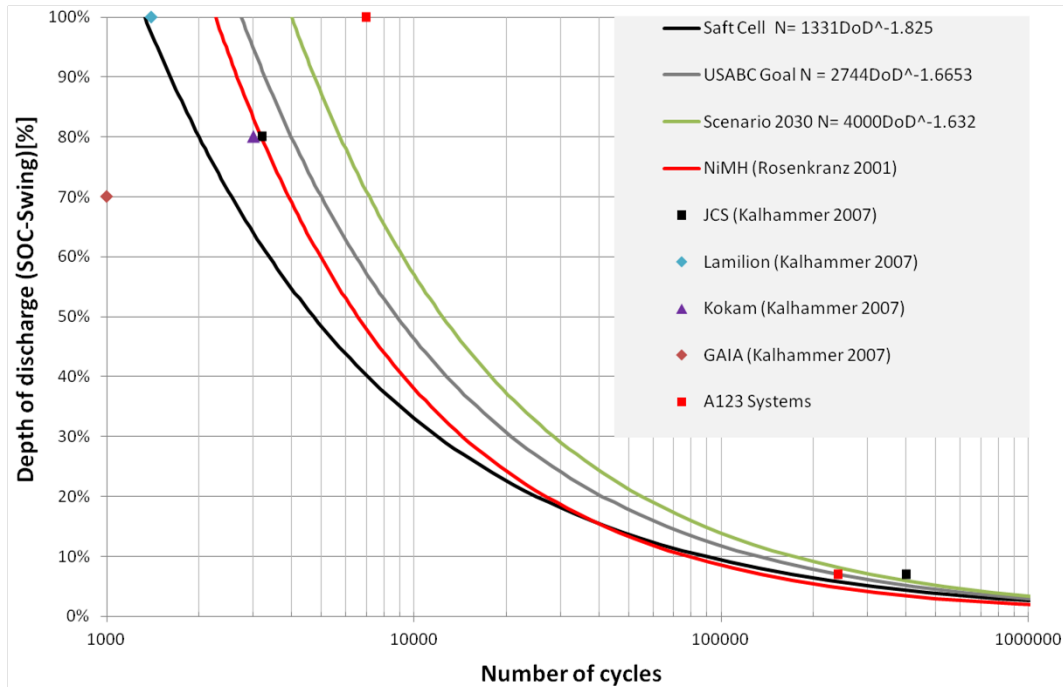


Figure 3-3: Battery cycle life dependent on the depth-of-discharge

Source: Own calculation using data from U.S. Advanced Battery Consortium (USABC) goal trend line [24]. From [29] for (DoD 70 % = 5,000 cycles and DoD 3 % = 1,000,000 cycles); Scenario 2030 own assumptions; NiMH function cycles = 1515 DoD^{-0.65} [32]; A123 System according to [29]; other cycle life data from [33].

The discussed model indicates the highest lifetime for a fully charged (100 % soc) battery without cycling. However, when considering calendar life, a soc of 100 % is the most demanding condition. This contradiction indicates a weakness of the model.

3.2.2 Model based on energy throughput

Cycle life and DoD do not seem to be appropriate approaches, especially for A123 Systems' batteries. Analyses in [29] show that the most important factor for capacity fade of A123 Systems is the energy processed and not the DoD, which is used in the equations above. According to the A123 Systems website, a cycle life of 7,000 cycles for a capacity fade of 20 % is assumed. This results in a lifetime reduction of 0.0029 percent points per cycle. [29] conclude that capacity fade per normalized Wh processed is 0.0062 percent points (maximum 2.85 C-rate) for driving and 0.0027 percent points (0.5 C-rate) for arbitrage. The

disparity of the two values is caused by different C-rates for driving and for arbitrage cycling.

3.2.3 Discharge costs

To decide whether V2G options are profitable, the battery degradation costs per unit discharge are required. When the battery is discharged, the degradation costs are a function $c_{dis}(DoD_{start}, DoD_{end})$, which depends on the DoD at the start of the discharging (DoD_{start}) and the DoD at the end (DoD_{end}). Additional parameters of the function are battery-specific parameters, the cost for the battery C_{bat} and the usable energy of the battery E_{bat} . The special case of regular charging and discharging up to a certain DoD is considered here, assuming that the degradation costs are equally distributed over all life cycles of the battery. In this case, the costs for one cycle, i.e. one discharge from $DoD_{start}=0$ to $DoD_{end}=DoD$, represent the total battery costs divided by the number of cycles.

$$c_{dis}(0, DoD) = \frac{C_{bat}}{N_{cycle}(DoD)} \quad (6)$$

The costs for one processed kWh illustrated in Figure 3-3 are given by Eq. 7.

$$c_{dis,energy}(0, DoD) = \frac{C_{bat} \cdot DoD \cdot E_{bat}}{N_{cycle}(DoD)} \quad (7)$$

It follows that the general degradation costs are:

$$c_{dis}(DoD_{start}, DoD_{end}) = c_{dis}(0, DoD_{end}) - c_{dis}(0, DoD_{start}) \quad (8)$$

for $DoD_{end} > DoD_{start}$

Then, the cost per discharge unit c_{dis_unit} as a function of the DoD before the discharge is:

$$\begin{aligned} c_{dis,unit}(DoD) &= c_{dis}(DoD, DoD+1\%) \\ &= c_{dis}(0, DoD+1\%) - c_{dis}(0, DoD) \\ &= \frac{C_{bat}}{N_{cycle}(DoD+1\%)} - \frac{C_{bat}}{N_{cycle}(DoD)} \end{aligned} \quad (9)$$

Figure 3-4 illustrates these specified discharge costs as a function of the DoD for the degradation functions described above, with specific investment costs of €247 per kWh of usable energy.

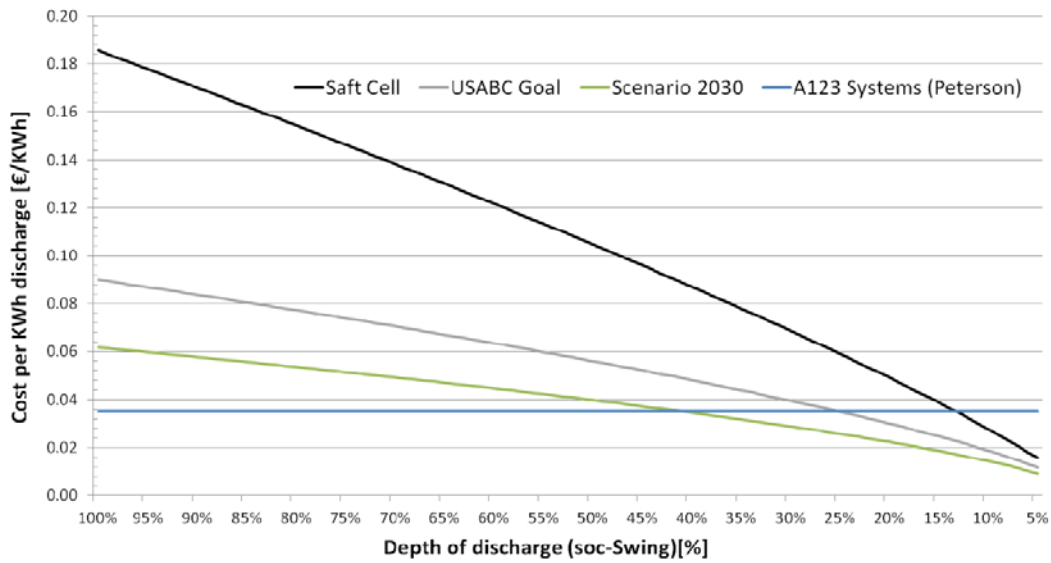


Figure 3-4: Battery degradation costs

Note: Investment 247 €/kWh of the usable energy for the battery system; costs caused by electricity losses due to V2G efficiencies are not included.

The cost calculation per energy unit discharged illustrates the necessary spread between the base price and the peak price for feeding electricity back into the grid. With the model based on the depth-of-discharge, the cost function rises with increasing DoD rates. For USABC and scenario 2030 assumptions, the costs per kWh are between 2 and 9 ct. The model based on the energy processed using the A123 battery performance results in constant costs of about 4 ct per kWh. The costs for a full cycle with the Saft cell are about 18 ct per kWh.

3.3 Optimization

The shortest path algorithm approach is used to find the optimal charging $d_{n,t}$ and discharging $s_{n,t}$ times for the operation schedule $w_{(0-T)}$ of a PEV n within the grid management time Δt_m [35]. Compared to a standard solver, this method allows a significant reduction in simulation time and high flexibility to integrate non-linear battery degradation costs [16, 17]. The implementation of the algorithm is explained below in a simplified example with the following boundary conditions.

- (1) State-of-charge: $soc_{t=0} = 80\%$; $soc_{t=4} = 100\%$
- (2) Increment of the storage: $\Delta soc = 10\%$
- (3) Grid connection power: $P = 4\text{kW}$, 1 kWh equals $\Delta soc = 10\%$
- (4) Optimization time period: $\Delta t_m = 4$
- (5) Charging efficiency: $\eta_{charge} = 100\%$

Define graph: For the specific problem, a graph Z is defined. $Z(\Delta t_m; E_{bat})$ consists of a set of finite vertices, in this case Δt_m with time steps t , and a set of finite edges given by the usable energy of the battery. For the vehicle embedded application of the algorithm, Δt_m is quarter-hourly resolved and depends on the standing time of the vehicle provided by the vehicle user. The battery state of charge is resolved in 0.25 kWh increments as an element of E_{bat} (usable battery storage 10 kWh). In the example, the optimization time is 4 time steps and the soc is divided into 10 increments (see Figure 3-5).

Weight edges: For all points in the graph $Z(\Delta t_m; E_{bat})$, the path to reach these points is assigned to the cost function:

$$\text{if } \Delta soc = 0 : c_t = 0 + c_{t-1} \quad (10)$$

$$\text{if } \Delta soc > 0 : c_t = p_{n,t} \cdot d_n \cdot t + c_{t-1}$$

$$\text{if } \Delta soc < 0 : c_t = -p_{n,t} \cdot s_{n,t} \cdot t + c_{dis}(\Delta soc) + c_{t-1}$$

The path with non-negative minimum costs to reach a point in $Z(\Delta t_m; E_{bat})$ is memorized. In the example, no discharging and a charging efficiency of 100% is assumed. Graph $Z(1,2,3,4;80\%,90\%,100\%)$ consists of all possible charging states over the optimization period. The electricity price $p_{n,t}$ and the calculated charging costs c_t for all paths to reach the final state are given in Tab 1.

Table 2-1: Overview of the renewable energy input data Example for the costs of all possible paths to reach the final state-of-charge

Path	Time Steps			
	1	2	3	4
1	0.22 €	0.37 €	0.37 €	0.37 €
2	0.22 €	0.22 €	0.36 €	0.36 €
3	0.22 €	0.22 €	0.22 €	0.47 €
4	0.00 €	0.15 €	0.29 €	0.29 €
5	0.00 €	0.15 €	0.15 €	0.40 €
6	0.00 €	0.00 €	0.14 €	0.39 €
Tariff (€/kWh)	0.22	0.15	0.14	0.25

Find shortest paths: After all the minimized costs have been calculated, the path or charging and discharging schedule which has the lowest costs to reach the final state-of-charge can be selected from the memorized values. For the presented example, paths 3 and 4 are shown in Figure 3-5. Here, path 4 provides the minimal charging costs to reach the final state-of-charge.

The optimization algorithm is called after each trip. Starting values are the actual $soc_{n,t}$ after the trip, the $soc_{n,\Delta t}$ to achieve and the time Δt_m to achieve the soc. For details on graph theory and shortest-path algorithms, see [36].

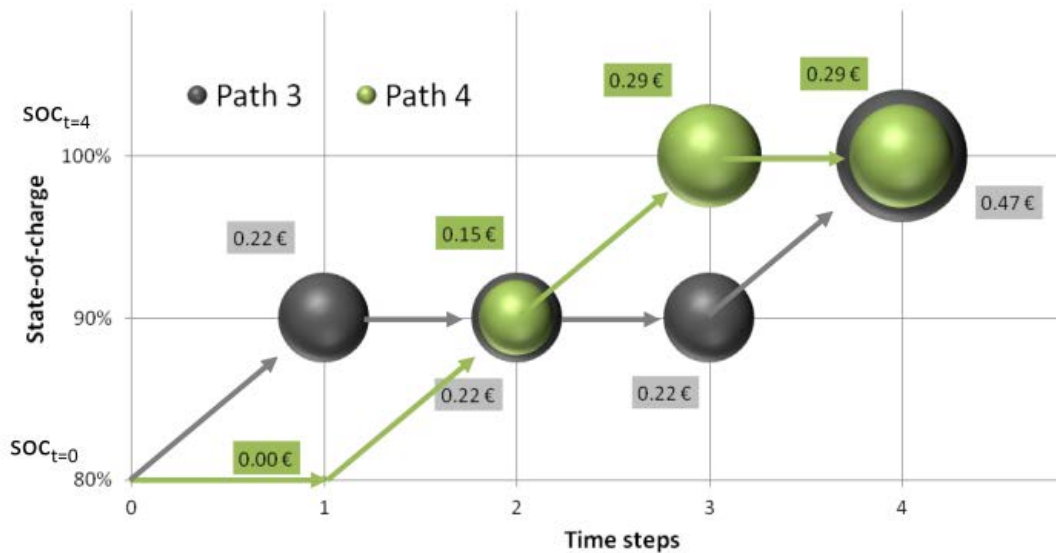


Figure 3-5: Examples of the path to reach the final state-of-charge

Note: The bubble size and the values represent the charging costs c_t .

4 Results

The result section focuses on how agent behavior differs depending on the methods used to calculate the battery degradation costs. Section 3.2 introduced two methods to calculate the discharging costs caused by battery degradation: discharging costs based on the energy processed and discharging costs based on the depth-of-discharge. Each method results in different agents' operation and V2G charging strategies, respectively. To compare the differences, a simulation was carried out with an agent using the method based on depth-of-discharge (DoD-agent) and another with an agent using the method based on energy throughput (Ah-agent). The following boundary conditions were applied for both agents: The simulation period is one week with a quarter-hourly time resolution. The tariff is based on our own assumptions and follows a typical day-and-night profile with a mid price period during the day, e.g. triggered by a high photovoltaic supply. The highest price spread between peak (during morning and evening hours) and base loads (during the night hours) is 8 ct/kWh. The tariff is designed to compare charging and discharging behavior. Therefore, the same tariff is used for all simulation days. For the case study, the following driving behavior is assumed. During the two first days (Sat and Sun) of the simulation, no driving is assumed. Afterwards, two daily 30 km trips, one in the morning (08:15) and one in the afternoon (16:45) are assumed. The energy use per trip is 6.3 kWh and the trip duration is 30 minutes or 2 time steps. The electricity tariff and the driving behavior used are shown in Figure 4-1.

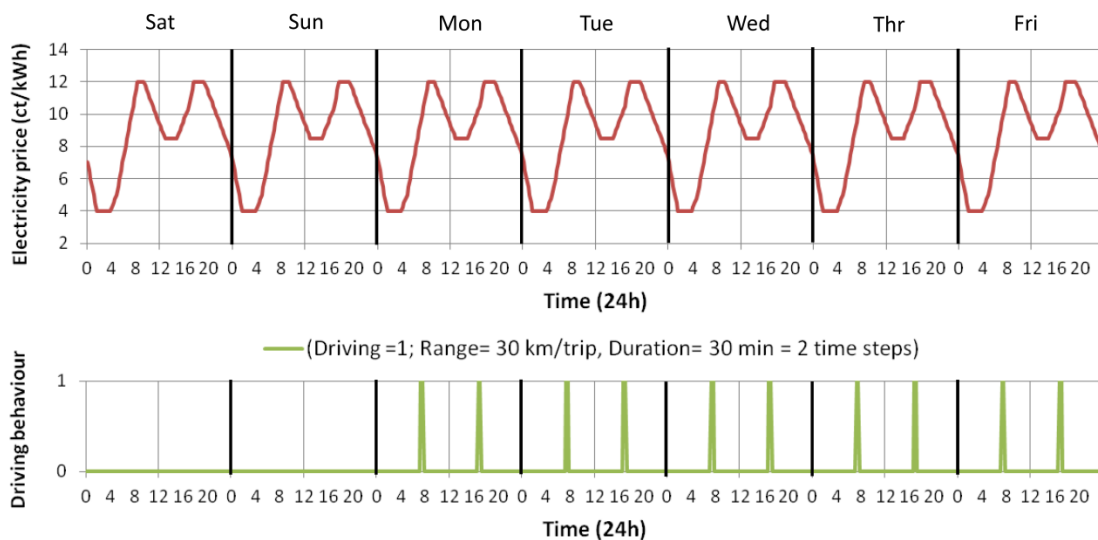


Figure 4-1: Electricity tariff and driving behavior

The usable storage of the agents' battery is 12 kWh. The discharging efficiency is 94 % and discharging cost parameters are $a = 7000$, $b = -1$ for the Ah-agent and $a = 4000$, $b = -1.632$ for the DoD-agent. The grid connection power is 4 kW, which allows a maximum charging energy of 1 kWh (8.33 % of soc) per time step. The optimization time period lies between the actual and the next trip and the beginning of the day to the next trip, respectively. The soc to be reached before a trip is set to 100 %.

The results of the one-week simulation are presented in Figure 4-2. During the first two days, both agents operate like a stationary storage device. The DoD-agent (upper part of Figure 4-2) uses the soc range of the battery only partly, whereas the Ah-agent uses the total soc range. In addition, a recharging of the DoD-agent can be observed. The recharging reduces the discharging costs for the next discharging cycle.

Including the driving behavior from Mon-Fri changes the V2G operation. Discharging during the day is no longer observed because the optimization period is only between the two trips and here the assumed tariff does not provide a period with the high and low prices necessary for a discharging cycle. After the second trip of the day, both agents start discharging. The cycle conducted by the DoD-agent again uses only a minimal soc of 39 % (4.7 kWh). In the case constructed here, the minimal soc of the agent used in a V2G cycle is constant because the price spread of the tariff is the same for all simulation days. The energy discharged in both cases is affected by driving behavior, but this effect is strongly enhanced when using the DoD-method.

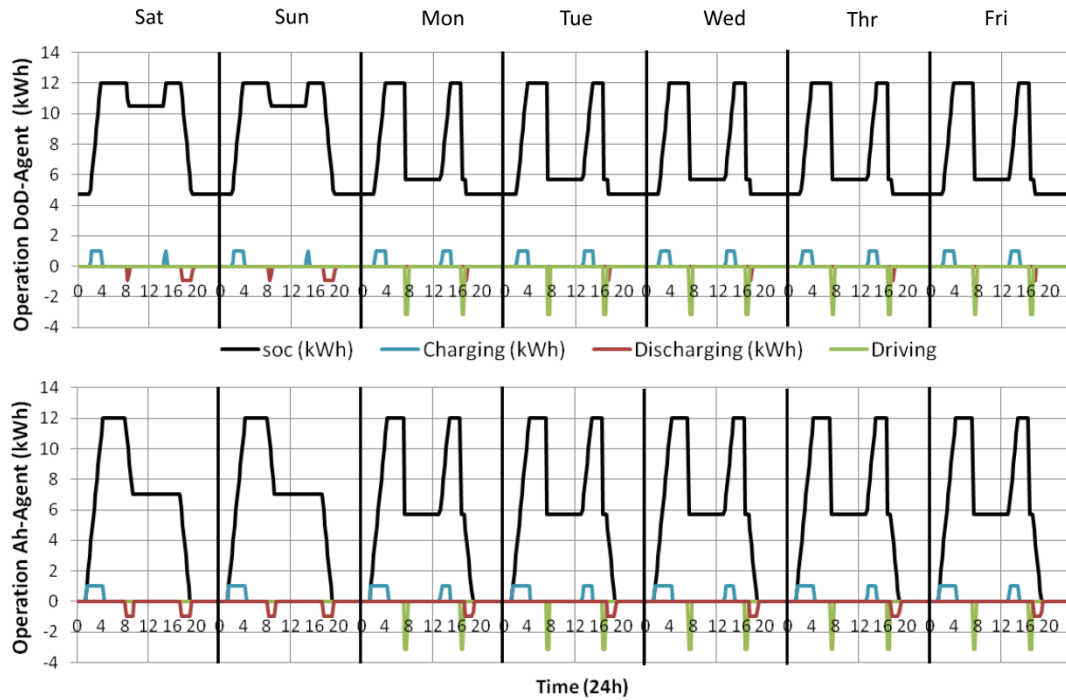


Figure 4-2: Operation behavior of agents

For a real vehicle or more realistic V2G power system analyses, the discussed effects of battery aging costs become far more complex. More realistic driving behavior with changing trip ranges and start times results in very different soc conditions and optimization time periods when returning from a trip. Furthermore, volatile electricity market prices with changing prices levels strongly influence the minimal soc applied of the DoD-agent.¹ Therefore, realistic discharging cost calculations should be included in V2G applications. The here discussed agents and the presented optimization algorithm provide the basis to implement different aging costs in simulation models as well as in real world V2G applications.

¹ A detailed analysis representing results for a system analysis of the German electricity market using the introduced agents is presented in [18].

5 Conclusions

This paper presented a method to simulate PEVs in electricity system models which considers individual driving behavior and battery discharging costs. The agent-based approach used also allows the same method to be used in vehicle embedded systems. This made it possible to test smart grid software applications in a simulation environment and investigate the effects of smart grid applications on the power system and the electricity market. It was also possible to use the introduced simulation model to analyze the value of a specific smart grid application and interrelations with other applications. This proves to be a main advantage of agent-based simulation, which permits a customized approach and can solve a complex problem while including control algorithms implemented in real smart grid applications.

6 Acknowledgements

This work has been co-financed by the German Federal Ministry for the Environment, Nature Conservation and Nuclear Safety (BMU) and E.ON AG within the project “Flottenversuch Elektromobilität”. We thank Martin Wietschel, Julius Richter and Gillian Bowman-Köhler for discussions and critical reading of the manuscript.


7 References

- [1] K. P. Schneider and J. C. Fuller. "Analysis of distribution level residential demand response." 2011 IEEE Power Systems Conference and Exposition (PSCE), pp. 1-6.
- [2] D. Nestle, „Energiemanagement in der Niederspannungsversorgung mittels dezentraler Entscheidung. -Konzept, Algorithmen, Kommunikation und Simulation.“ Ph.D Dissertation, Institute of Energy Engineering. Department of Efficient Energy Conversion. University of Kassel, Kassel, 2007.
- [3] J. A. Peças Lopes, S. A. Polenz, C. L. Moreira and R Cherkaoui, "Identification of control and management strategies for LV unbalanced microgrids with plugged-in electric vehicles". *Electric Power Systems Research* 80 (8): 898-906, 2010.
- [4] S. D. J. McArthur, SDJ and E. M. Davidson, "Multi-Agent Systems for Power Engineering Applications — Part I : Concepts , Approaches , and Technical Challenges". *Power Systems* 22 (4): 1743-1752, 2007.
- [5] S. D. J. McArthur, SDJ and E. M. Davidson, "Multi-Agent Systems for Power Engineering Applications — Part II : Technologies , Standards , and Tools for Building Multi-agent Systems". *Power Systems* 22 (4): 1753-1759, 2007.
- [6] R. Roche, B. Blunier, A. Miraoui, V. Hilaire and A. Koukam, "Multi-agent systems for grid energy management: A short review." Paper presented at IECON 2010 - 36th Annual Conference on IEEE Industrial Electronics Society, Phoenix, November 7-10, 2010.
- [7] J. K. Kok and M. J. J. Scheepers, "Intelligence in electricity networks for embedding renewables and distributed generation." In *Intelligent Infrastructures, Intelligent Systems, Control and Automation: Science and Engineering Volume 42* edited by Negenborn, RR, Z Lukszo, and H Hellendoorn, Springer, 2010.
- [8] J. M. Akkermans and J. Schreinemakers, "Microeconomic distributed control: Theory and application of multi-agent electronic markets." In *Proceedings of CRIS* (ii): 1-8, 2004. Available: http://www.see.asso.fr/clubs_techniques/se/xmedia/Club_Tech_SE-2001-2008/2004/CRIS-Grenoble-10-04/S8/s8-a1.pdf

- [9] B. Roossien, "Field-test upscaling of multi-agent coordination in the electricity grid." Paper presented at 20th International Conference and Exhibition on Electricity Distribution (CIRED) - Part 1, Prague, June 8-11, 2009.
- [10] S. Ramchurn, P. Vytelingum and A. Rogers, "Agent-based control for decentralised demand side management in the smart grid." Paper presented at Proc. of 10th Int. Conf. on Autonomous Agents and Multiagent Systems – Innovative Applications Track (AA- MAS), Taipei, 02 – May 06, 2011.
- [11] M. Fahrioglu, "Designing incentive compatible contracts for effective demand management". IEEE Transactions on Power Systems 15 (4): 1255-1260, 2000.
- [12] Z. Fan, "Distributed charging of PHEVs in a smart grid." Paper presented at IEEE Second International Conference on Smart Grid Communications, Brussels, October 17 - 20, 2011.
- [13] Wu, C, H Mohsenian-Rad, and J Huang. 2012. Vehicle-to-aggregator interaction game. IEEE Transactions on Smart Grid 3 (1): 434-442.
- [14] M. Galus, and G. Andersson, "Demand Management of Grid Connected Plug-In Hybrid Electric Vehicles (PHEV)". IEEE Energy 2030 Conference (November): 1-8, 2008.
- [15] N. Rotering and M. Illic, "Optimal charge control of plug-in hybrid electric vehicles in deregulated electricity markets". IEEE Transactions on Power Systems 26 (3): 1021-1029, 2010.
- [16] J. Link, M. Büttner, D. Dallinger, and J. Richter, "Optimisation Algorithms for the Charge Dispatch of Plug-in Vehicles based on Variable Tariffs." Working paper sustainability and innovation No. S3/2010, 2010. Available: <http://econstor.eu/bitstream/10419/36697/1/623961075.pdf>.
- [17] J. Link, "Elektromobilität und erneuerbare Energien: Lokal optimierter Einsatz von netzgekoppelten Fahrzeugen." Phd Dissertation., Department of Electrical Engineering and Information Technology, Technical University Dortmund, Dortmund, 2011.
- [18] D. Dallinger, "Plug-in electric vehicles integrating fluctuating renewable electricity," Phd Dissertation., Department of Electrical Engineering and Computer Science, University Kassel, Kassel, 2013.

- [19] M. Wooldridge, "An Introduction to MultiAgent Systems" -1st edition, Chichester: John Wiley & Sons, 2002.
- [20] D. Dallinger and M. Wietschel, "Grid integration of intermittent renewable energy sources using price-responsive plug-in electric vehicles". *Renewable and Sustainable Energy Review* 16 (5): 3370-3382, 2012.
- [21] S. Schey, D. Scofield and J. Smart, "A First Look at the Impact of Electric Vehicle Charging on the Electric Grid in The EV Project". Paper presented at 26th Electric Vehicle Symposium (EVS-26), Los Angeles, May 6-9, 2012.
- [22] J. S. Rosenschein and G. Zlotkin, "Ruels of Encounter: Designing conventions for automated negotiation among computers". Cambridge: MIT Press, 1994.
- [23] F. Sensfuß, "Assessment of the impact of renewable electricity generation on the German electricity sector - An agent-based simulation approach." Phd Dissertation, Karlsruhe Institute of Technology, Karlsruhe, 2007.
- [24] USABC: U.S. Advanced Battery Consortium, "Electric vehicle battery test procedure manual." Tech. Rep., 1996. Available: http://avt.inel.gov/battery/pdf/usabc_manual_rev2.pdf.
- [25] P. Ramadass, B. Haran, R. White and B. N. Popov, "Capacity fade of Sony 18650 cells cycled at elevated temperatures Part I . Cycling performance". *Journal of Power Sources* 112: 606-613, 2002.
- [26] K. Smith, G. H- Kim and A. Pesaran, "Modeling of Nonuniform Degradation in Large-Format Li-ion Batteries." Poster National Renewable Energy Laboratory, 2009. Available: <http://www.nrel.gov/vehiclesandfuels/energystorage/pdfs/46041.pdf>.
- [27] D. U. Sauer, and H Wenzl, "Comparison of different approaches for life-time prediction of electrochemical systems—Using lead-acid batteries as example". *Journal of Power Sources* 176 (2): 534-546, 2008.
- [28] R. B. Wright, C. G. Motloch and J. R. Belt, "Calendar-and cycle-life studies of advanced technology development program generation 1 lithium-ion batteries". *Journal of Power* 110: 445-470, 2002.

- [29] S. B. Peterson, J. Apt, and J. F. Whitacre, "Lithium-ion battery cell degradation resulting from realistic vehicle and vehicle-to-grid utilization". *Journal of Power Sources* 195 (8): 2385-2392, 2009.
- [30] G. Ning and B. N- Popov, "Cycle Life Modeling of Lithium-Ion Batteries". *Journal of The Electrochemical Society* 151 (10): A1584, 2004.
- [31] G. Sarre, P. Blanchard and M. Broussely, "Aging of lithium-ion batteries". *Journal of Power Sources* 127 (1-2): 65-71, 2004.
- [32] K. Rosenkranz, "Deep-Cycle Batteries for Plug-in Hybrid Application", Paper presented at 20th Electric Vehicle Symposium (EVS-20), Plug-In Hybrid Vehicle Workshop, Long Beach, November 15-19, 2003.
- [33] F. R. Kalhammer, B. M. Kopf, D. H. Swan, V. P. Roan and M. P. Walsh, "Status and prospects for zero emissions vehicle technology", Report of the ARB Independent Expert Panel 2007. Prepared for State of California Air Resources Board Sacramento, California, 2007. Available: www.arb.ca.gov/msprog/zevprog/zevreview/zev_panel_report.pdf.
- [34] A. A. Pesaran, T. Markel, H. S. Tataria and D. Howell, "Battery requirements for plug-in hybrid electric vehicles – analysis and rationale." Paper presented at 23rd Electric Vehicle Symposium (EVS-23), Anaheim, December 2-5, 2007. Available: http://www.spinovation.com/sn/Batteries/Battery_Requirements_for_Plug-In_Hybrid_Electric_Vehicles_-_Analysis_and_Rational.pdf
- [35] E. W. Dijkstra, "A note on two problems in connexion with graphs". *Numerische Mathematik* 1 (1): 269-271, 1959.
- [36] A. Gibbons, *Algorithmic Graph Theory*. Cambridge University Press. pp. 5–6, 1985.



Authors' affiliations

David Dallinger

Fraunhofer Institute for Systems and Innovation Research (Fraunhofer ISI)

Jochen Link and Markus Büttner worked for the Fraunhofer Institute for Solar Energy Systems, Freiburg, Germany, while contributing to this paper.

Contact: Brigitte Kallfass

Fraunhofer Institute for Systems
and Innovation Research (Fraunhofer ISI)
Competence Center Energy Policy and Energy Markets
Breslauer Strasse 48
76139 Karlsruhe
Germany
Phone: +49 / 721 / 6809-150
Fax: +49 / 721 / 6809-203
E-mail: brigitte.kallfass@isi.fraunhofer.de
URL: www.isi.fraunhofer.de

Karlsruhe 2013